The American Journal of Sports Medicine

BioCartilage Improves Cartilage Repair Compared With Microfracture Alone in an Equine Model of Full-Thickness Cartilage Loss

Lisa A. Fortier, Hannah S. Chapman, Sarah L. Pownder, Brandon L. Roller, Jessica A. Cross, James L. Cook and Brian J. Cole

Published by:
$SAGE

http://www.sagepublications.com

On behalf of:

American Orthopaedic Society for Sports Medicine

AOSSM

Additional services and information for **The American Journal of Sports Medicine** can be found at:

Email Alerts: http://ajs.sagepub.com/cgi/alerts

Subscriptions: http://ajs.sagepub.com/subscriptions

Reprints: http://www.sagepub.com/journalsReprints.nav

Permissions: http://www.sagepub.com/journalsPermissions.nav

>> Version of Record - Sep 1, 2016

OnlineFirst Version of Record - Jun 13, 2016

What is This?

BioCartilage Improves Cartilage Repair Compared With Microfracture Alone in an Equine Model of Full-Thickness Cartilage Loss

Lisa A. Fortier,* DVM, PhD, Hannah S. Chapman,* DVM, Sarah L. Pownder,[†] DVM, Brandon L. Roller,[‡] MD, PhD, Jessica A. Cross,* BS, James L. Cook,[§] DVM, PhD, and Brian J. Cole,[‖¶] MD, MBA
Investigation performed at Cornell University, Ithaca, New York, USA

Background: Microfracture (MFx) remains a dominant treatment strategy for symptomatic articular cartilage defects. Biologic scaffold adjuncts, such as particulated allograft articular cartilage (BioCartilage) combined with platelet-rich plasma (PRP), offer promise in improving clinical outcomes as an adjunct to MFx.

Purpose: To evaluate the safety, biocompatibility, and efficacy of BioCartilage and PRP for cartilage repair in a preclinical equine model of full-thickness articular cartilage loss.

Study Design: Controlled laboratory study.

Methods: Two 10-mm-diameter full-thickness cartilage defects were created in 5 horses in the trochlear ridge of both knees: one proximal (high load) and another distal (low load). Complete blood counts were performed on each peripheral blood and resultant PRP sample. In each horse, one knee received MFx with BioCartilage + PRP, and the other knee received MFx alone. Horses were euthanized at 13 months. Outcomes were assessed with serial arthroscopy, magnetic resonance imaging (MRI), micro–computed tomography (micro-CT), and histology. Statistics were performed using a mixed-effects model with response variable contrasts.

Results: No complications occurred. PRP generated in all subjects yielded an increase in platelet fold of 3.8 ± 4.7. Leukocyte concentration decreased in PRP samples by an average fold change of 5 ± 0.1. The overall International Cartilage Repair Society repair score in both the proximal and distal defects was significantly higher (better) in the BioCartilage group compared with MFx (proximal BioCartilage: 7.4 ± 0.51, MFx 4.8 ± 0.1, $P = .041$; distal BioCartilage: 5.6 ± 0.98, MFx 2.6 ± 1.5, $P = .022$). BioCartilage-treated proximal defects demonstrated improved histologic scores for repair-host integration (BioCartilage, 96 ± 9; MFx, 68 ± 18; $P = .02$), base integration (BioCartilage, 100 ± 0; MFx, 70 ± 37; $P = .04$), and formation of collagen type II (BioCartilage, 82 ± 8; MFx, 58 ± 11; $P = .05$) compared with the positive control. On MRI, T2 relaxation time was significantly shorter (better) in the superficial region of BioCartilage-treated distal defects compared with MFx ($P = .05$). There were no significant differences between BioCartilage and MFx on micro-CT analysis.

Conclusion: BioCartilage with PRP safely improved cartilage repair compared with MFx alone in an equine model of articular cartilage defects up to 13 months after implantation.

Clinical Relevance: The 1-year results of BioCartilage + PRP suggest that homologous allograft tissue provides a safe and effective augmentation of traditional MFx.

Keywords: knee; articular cartilage; BioCartilage; marrow stimulation procedures; platelet-rich plasma

The regenerative capacity of adult cartilage is negligible.[1] Cartilage procedures are the most commonly performed knee arthroscopic surgeries, with rates increasing by 5% annually among privately insured US residents alone.[7] Given such high prevalence, improving current treatment options to involve single-stage procedures with consistently good long-term outcomes is vital. Marrow stimulation procedures, primarily in the form of microfracture (MFx), have become a mainstay treatment for small (<2.5 cm²) focal chondral defects refractory to nonsurgical management. By penetrating the subchondral bone with perpendicular holes placed 2 to 3 mm apart, MFx allows pluripotent bone marrow stem cells to fill the defect, form a fibrin plug, and differentiate into fibrocartilage-producing cells.[12] While MFx has yielded positive outcomes

at 2-year follow-up in younger (<30 years) populations with small cartilage defects, the procedure has several limitations. A recent systematic review showed that knee function scores deteriorated after 2 years after MFx, with only 67% to 85% of patients reporting positive outcomes between 2 and 5 years.[8] Further limitations include lack of hyaline cartilage fill, unpredictable volume of fibrocartilage fill, poorer outcomes for larger defects, subchondral bone advancement (internal osteophyte formation) in defects, and higher failure rates for cell-based approaches in patients with previous MFx.[10] Given these limitations, there has been increased interest in improving the MFx technique. Thus far, trials augmenting MFx with stem cells, growth factors, and cell scaffolds have all produced encouraging results.[13,15]

BioCartilage (Arthrex Inc) contains desiccated, particulated allograft cartilage that is hydrated with platelet-rich plasma (PRP) and placed into contained cartilage defects where MFx has been performed. The purpose of this investigation was to evaluate the safety, biocompatibility, and efficacy of BioCartilage and leukocyte-reduced PRP for cartilage repair in a preclinical equine lateral femoral trochlear ridge model of full-thickness articular cartilage loss.

METHODS

All procedures were approved by the Cornell University Animal Care and Use Committee. Five adult horses (age range, 2-5 years) were included in the study. Lameness examinations were performed, and 3-view patellofemoral joint radiographs were obtained preoperatively, at 2- and 6-month recheck arthroscopies, and before euthanasia at 13 months. Horses were placed under general anesthesia and were routinely prepared for arthroscopic surgery of the patellofemoral joint. Before surgery, synovial fluid was aspirated for differential nucleated cell counts and total protein measurements. Synovial fluid was also obtained at 14 days, 1 month, 2 months, and 13 months after surgery and similarly analyzed as a measure of inflammation/synovitis in the joints. Blood was aspirated from the jugular vein to generate PRP according to manufacturer directions (Autologous Conditioned Plasma; Arthrex Inc). Nucleated cell and platelet counts were performed on samples of blood and PRP from each horse.

Using a standard arthroscopic approach to the lateral trochlear ridge of the femur, two 10-mm-diameter, full-thickness cartilage defects were created approximately 1 cm apart using a drill bit with a cannula that was designed to allow 2 mm of drilling depth to remove the articular cartilage but not penetrate the subchondral bone plate. The proximal defect was made with the limb in full extension and instrumentation introduced at the base of the patella. The joint was then flexed to allow creation of a defect 1 cm distal to the first lesion. The remaining calcified cartilage was removed with a Cobb elevator. Limbs were randomized either to MFx with BioCartilage suspended in PRP or to MFx alone. Both defects in each limb received the same treatment, with the opposite limb serving as the contralateral control, so that the effects of high (proximal defect) and low (distal defect) loading on repair tissue could be assessed. For each of the 2 defects in the BioCartilage limbs, 6 MFx perforations were made, CO_2 gas arthroscopy was used to dry the defect, and BioCartilage + PRP was delivered using a 10-G needle to a level slightly below the surrounding cartilage. A 1:0.8 combination of BioCartilage and PRP was mixed and delivered into the defect.[2] The BioCartilage graft was sealed with fibrin sealant (Tisseel; Baxter Healthcare Corp) to create a surface level with the surrounding cartilage. When both defects were grafted, gas arthroscopy was discontinued, fluid was reintroduced, and the joint was put through range of motion to confirm graft retention. In the control limb, MFx alone was performed. Horses were recovered from anesthesia and rested for 2 weeks. Exercise was restricted to 30 minutes of walking per day until recheck arthroscopy at 2 months postoperatively.

Recheck Arthroscopic Surgeries

Routine arthroscopy of the patellofemoral joints and International Cartilage Repair Society (ICRS) scoring were performed by consensus scoring of 2 experienced orthopaedic surgeons, blinded to the treatment groups, in anesthetized horses at 2, 6, and 13 months postoperatively (Table 1). Horses were rested for 10 days and then allowed free exercise in a pasture. At 13 months, horses were euthanized, and arthroscopy with ICRS scoring was repeated. The joints were then disarticulated and transported on ice to the Hospital for Special Surgery for 3-T magnetic resonance imaging (MRI) evaluation.

¶Address correspondence to Brian J. Cole, MD, MBA, Midwest Orthopaedics at Rush, 1611 W Harrison Street, Suite 300, Chicago, IL 60612 (email: cole.research@rushortho.com).

*Department of Clinical Sciences, Cornell University, Ithaca, New York, USA.
†MRI Laboratory, Hospital for Special Surgery, New York, New York, USA.
‡Arthrex Inc, Naples, Florida, USA.
§Comparative Orthopaedic Laboratory, University of Missouri, Columbia, Missouri, USA.
‖Division of Sports Medicine, Rush University Medical Center, Chicago, Illinois, USA.

TABLE 1
Modified International Cartilage Repair Society Scoring System
Used to Evaluate Repair Tissue During Arthroscopic Surgery

	Score				
	0	1	2	3	4
% defect repair	0% repair of defect depth	25% repair of defect depth	50% repair of defect depth	75% repair of defect depth or proud	Level with surrounding cartilage
Integration	From no contact to $1/4$ of graft integrated with surrounding cartilage	$1/2$ of graft integrated with surrounding cartilage, $1/2$ with a notable boarder >1 mm	$3/4$ of graft integrated, $1/4$ with a notable border >1 mm width	Demarcating border <1 mm	Complete integration with surrounding cartilage
Macroscopic	Total degeneration of grafted are	Several small or few but large fissures	Small, scattered fissures or cracks	Fibrillated surface	Intact, smooth surface
Patella	Grade 4: severely abnormal	Grade 3: abnormal	Grade 2: nearly normal	Grade 1: normal	Not assigned
Synovial membrane	Grade 4: severely abnormal	Grade 3: abnormal	Grade 2: nearly normal	Grade 1: normal	Not assigned

MRI

All scanning was performed on a clinical 3-T MRI scanner (GE Healthcare) with an 8-channel phased-array knee coil (Invivo). MRI scanning and scoring were performed by radiologists blinded to the treatment group. Morphologic sagittal and axial plane 2-dimensional (2D) fast spin-echo (FSE) images were acquired (echo time [TE], 21 ms; repetition time [TR], 4000 ms; receiver bandwidth [RBW], ±62.5 kHz; acquisition matrix [AM], 512 × 416; number of excitations [NEX], 2-3; field of view [FOV], 14 × 14 cm; slice thickness [SL], 2.0 mm; slice spacing [SS], 0 mm). Quantitative 2D T2 mapping of articular cartilage as a measure of collagen content and orientation was performed (parameters: TR, 1000 ms; 8 TEs, 7.4-59.5 ms; SL, 2.5 mm; FOV, 14 cm; AM, 384 × 256; RBW, ±62.5 kHz). Three-dimensional (3D) T1ρ imaging assessed relative proteoglycan content within the reparative tissue (parameters: TE, 2.3 ms; TR, 6.3 ms; spin-lock time [TSL], 0, 20, 40, 60 ms; FOV, 14 cm; AM, 256 × 160; slice thickness, 2.5 mm; BW, ±41.7 kHz; views per segment, 24; spin lock frequency, 500 Hz; NEX, 0.68).

Quantitative T2 and T1ρ values were calculated on a pixel-by-pixel basis by fitting the TE or TSL to the corresponding signal intensity data (Functool 3.1; GE Healthcare) using a mono-exponential decay equation: $SI(TE) \approx \exp(-TE/T2)$ and $SE(TSL) \approx \exp(-TSL/T1\rho)$, respectively. Regions of interest were obtained in both superficial and deep regions of the following areas: (1) center of the cartilage repair, (2) lateral and medial interfaces of the repair, and (3) native cartilage. The morphologic FSE images were assessed for (1) bony overgrowth (absence or presence), (2) percentage of fill based on both axial and sagittal images (0%-33%, 34%-65%, and 66%-100%), (3) integrity of the subchondral bone (intact or not intact), (4) sclerosis (none, mild, moderate, and severe), (5) integration (yes or no), and (6) morphology (flush, partial-thickness defect, or full-thickness defect).

Gross Assessment

After MRI, patellofemoral joints were opened and photographed. Gross observations of the trochlear cartilage, synovial membrane, and patellar surface were recorded. Repair tissue was scored by blinded observers, applying the same modified ICRS scoring system used during arthroscopy. A sample of synovial membrane was obtained and fixed in 4% paraformaldehyde. Osteochondral sections were cut to include 1 cm of normal cartilage on each side of the repair tissue and 1 cm of subchondral bone. Osteochondral blocks were fixed in 4% paraformaldehyde and stored in phosphate-buffered saline for micro–computed tomography (micro-CT).

Micro-CT

Micro-CT scans of osteochondral blocks were acquired using a GE eXplore CT 120 micro-CT scanner (GE Healthcare) with a current of 50 mA, voltage of 100 kVp, exposure time of 20 milliseconds, and acquisition resolution of 50 μm. Each scan consisted of 720 projections in a single full rotation of the gantry. Two frames were acquired at each position of the gantry and averaged before being transferred to the workstation for reconstruction. Micro-CT scans were imported into GEHC MicroView (Microview v. 2.3.a7) to create a 3D representation of the data for measurements of (1) trabecular thickness (average thickness of bone trabecula), (2) trabecular spacing (average separation between trabecula), (3) bone volume/tissue volume, (4) connectivity (density of trabecular connections), and (5) central osteophyte volume within a user-defined 3D region of interest for each defect. Evaluators were blinded to treatment groups throughout the analyses. Gray values, equivalent to the degree of bone mineralization, were plotted on a histogram, and the threshold was defined as the minimum in the histogram distribution, separating bone from marrow and soft tissue. Connectivity

TABLE 2
Synovial Membrane Histologic Scoring Rubric

	Score			
	0	1	2	3
Villus architecture	Normal shape	Slight clubbing	Moderate clubbing	Severe clubbing
Subintimal fibrosis	Normal	Slight increase	Moderate increase	Severe increase
Intimal layer thickness	Normal (1-2 layers thick)	3-4 layers thick	5-6 layers thick	7 layers or greater
Vasculature (number of vessels)	Normal	Slight increase	Moderate increase	Severe increase
Inflammatory cell infiltrate (perivascular cuffing)	Normal/none	Slight increase	Moderate increase	Severe increase

(number of trabecular connections/mm^3) was derived from the Euler number and is a topological measure used to describe the porosity of a bone sample, quantifying branching of the bone tissue structure. Trabecular thickness (mm) was defined as the average bone thickness and was calculated as the average thickness of all bone voxels. Trabecular spacing (mm) is the average bone separation, or the thickness of cavities. Osteophyte volume was defined as the volume of tissue protruding from the subchondral bone in the defect toward the articular surface, for which the gray values were equal to or greater than that of the defined threshold. The total volume of tissue classified as osteophyte (in mm^3) was determined based on the known voxel volume.

Histology

After micro-CT, osteochondral blocks from each of the 2 repair sites in both limbs were decalcified in 10% ethylenediaminetetraacetic acid solution then processed for histology, embedded in paraffin, and sectioned at 6 to 8 μm. Sections were stained with hematoxylin and eosin (H&E) or safranin O–fast green, and immunohistochemistry was performed for collagen type II. Synovial membrane samples were stained with H&E and scored for evidence of fibrosis or inflammation (Table 2). Osteochondral sections were scored using the ICRS II for Osteochondral Repair histology scoring system,[5] modified to include assessment of subchondral bone integrity (Table 3). All histologic sections were viewed using a dual-view microscope with 2 authors discussing and then generating a consensus score.

Statistical Analysis

For measures of cartilage repair (arthroscopic scores, MRI, histology), a mixed-effect model was fitted to the data, with horse treated as a random effect, site (distal or proximal) and treatment (MFx control or BioCartilage treatment) treated as fixed effects, and an interaction term for defect site × treatment. Linear contrasts were used to test differences between pairs of specific interest. Categorical (yes/no) histologic osteophyte data were analyzed using a Fisher exact test. A paired t test was performed on synovial membrane histology scores and synovial fluid cytology scores for nucleated cell counts and total protein concentration. Statistical analysis was performed using JMP (SAS

Institute) with $P < .05$ considered significant. Effect size was calculated for significant findings.

RESULTS

Peripheral Blood Analysis

PRP was generated from the blood of all subjects as defined by an increase in platelet concentration in PRP compared with blood. The average fold increase in platelets was 3.8 ± 4.7. Leukocyte concentration decreased in PRP samples by an average fold change of 5 ± 0.1.

Synovial Fluid Analysis

There were no intra- or postoperative complications in either the MFx or BioCartilage repair procedures. At all time points evaluated (time 0, 14 days, 1 month, 2 months, and 13 months), there were no significant differences in nucleated cell counts or total protein concentration between MFx and BioCartilage groups (all $P > .10$). Nucleated cell counts and total protein concentration approximately doubled in the day 14 samples but returned to normal/time 0 values by 30 days after surgery. This suggests that neither BioCartilage nor PRP resulted in inflammatory responses that were any greater than for surgery and MFx alone.

Arthroscopic Evaluation of Repair Tissue

The overall repair score at 13 months was significantly better (higher) in BioCartilage-treated repair sites compared with MFx in both proximal ($P = .04$, Cohen $d = 1.16$, effect size = 0.50) and distal ($P = .02$, Cohen $d = 1.07$, effect size = 0.47) defects (Figures 1 and 2). There were no significant differences in repair tissue scores between BioCartilage and MFx in either proximal or distal defects at 2- or 6-month recheck arthroscopies ($P = .23$-.55).

The articular surface of the patella was evaluated, and included in the composite overall arthroscopic score, at each arthroscopy to assess for potential detrimental effects of BioCartilage/PRP grafting on the opposing articular surface. There was no significant difference due to treatment at any time point for patellar cartilage ($P > .53$). The synovial membrane was also examined at each arthroscopy for signs of increased vascularity or fibrosis. There were no

TABLE 3
Modified International Cartilage Repair Society Scoring System for Cartilage Repair

Stain	Histologic Parameter[a]		Score[b]
Safranin O–fast green	Surface/superficial architecture	Cartilage	Defect
			Adjacent
	Inflammatory cell infiltrate	Cartilage	Defect
			Adjacent
	Vascularization	Cartilage	Defect
			Adjacent
	Repair-host integration	Cartilage	Defect
	Basal neocartilage-bone integration	Cartilage	Defect
	Surface/superficial assessment	Cartilage	Defect
			Adjacent
	Mid/deep zone assessment	Cartilage	Defect
			Adjacent
	Overall assessment	Cartilage	Defect
			Adjacent
	Matrix staining (metachromasia)	Cartilage	Defect
			Adjacent
	Calcification/ossification	Cartilage	Defect
			Adjacent
	Central osteophyte extending into deep zone of cartilage defect	Cartilage	Defect
	Central osteophyte extending into the superficial zone of cartilage defect	Cartilage	Defect
	Subchondral bone plate	Bone	Defect
			Adjacent
	Presence of epiphyseal/subchondral bone cyst (with secretory lining), yes/no	Bone	Defect
			Surrounding
	Presence of bone void (with or without fibrovascular tissue and without secretory lining), yes/no	Bone	Subchondral
Immunohistochemistry	C2: type II collagen	Cartilage	Defect
			Adjacent

[a]*Adjacent* is defined as the surface of the cartilage 2 mm surrounding the defect, *defect* as the area of the original cartilage defect, and *surrounding* as the sides and bottom of the defect.
[b]Scores are assigned on a 0-100 scale, with 100 being normal.
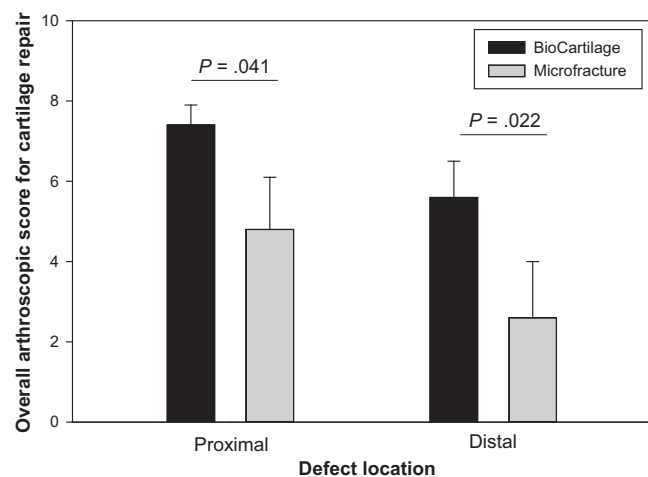

Figure 1. Arthroscopy scores of repair tissue in proximal and distal cartilage defects 13 months after grafting with BioCartilage + platelet-rich plasma after microfracture or treatment with microfracture alone. Repair tissue was significantly better in both proximal (high-load) and distal (low-load) sites compared with cartilage defects treated with microfracture alone.

significant differences between the 2 groups at any time point ($P > .25$). This supports the synovial fluid analysis results that BioCartilage grafting is not associated with adverse inflammatory responses beyond those induced by arthroscopic surgery with MFx alone.

MRI Evaluation

No cartilage hypertrophy or repair site displacement was seen for any defect site. In all horses, each BioCartilage- and MFx-treated repair site demonstrated mixed signal intensity, consistent with immature repair cartilage (Figure 2). There were no significant differences in MRI scores for sclerosis, proud bone, percentage defect fill, subchondral plate, morphology, integration, or total score between BioCartilage or MFx in either proximal or distal defects ($P = .18$-1.0). No defect was deemed free of sclerosis. For T2 and T1ρ mapping, superficial and deep zones of repair tissue within each proximal and distal defect were evaluated. T2 relaxation time was significantly shorter (better) in the superficial region of BioCartilage-treated distal defects compared with MFx ($P = .05$). There were no significant differences in T1ρ mapping between BioCartilage and MFx repair tissues ($P = .10$-.73).
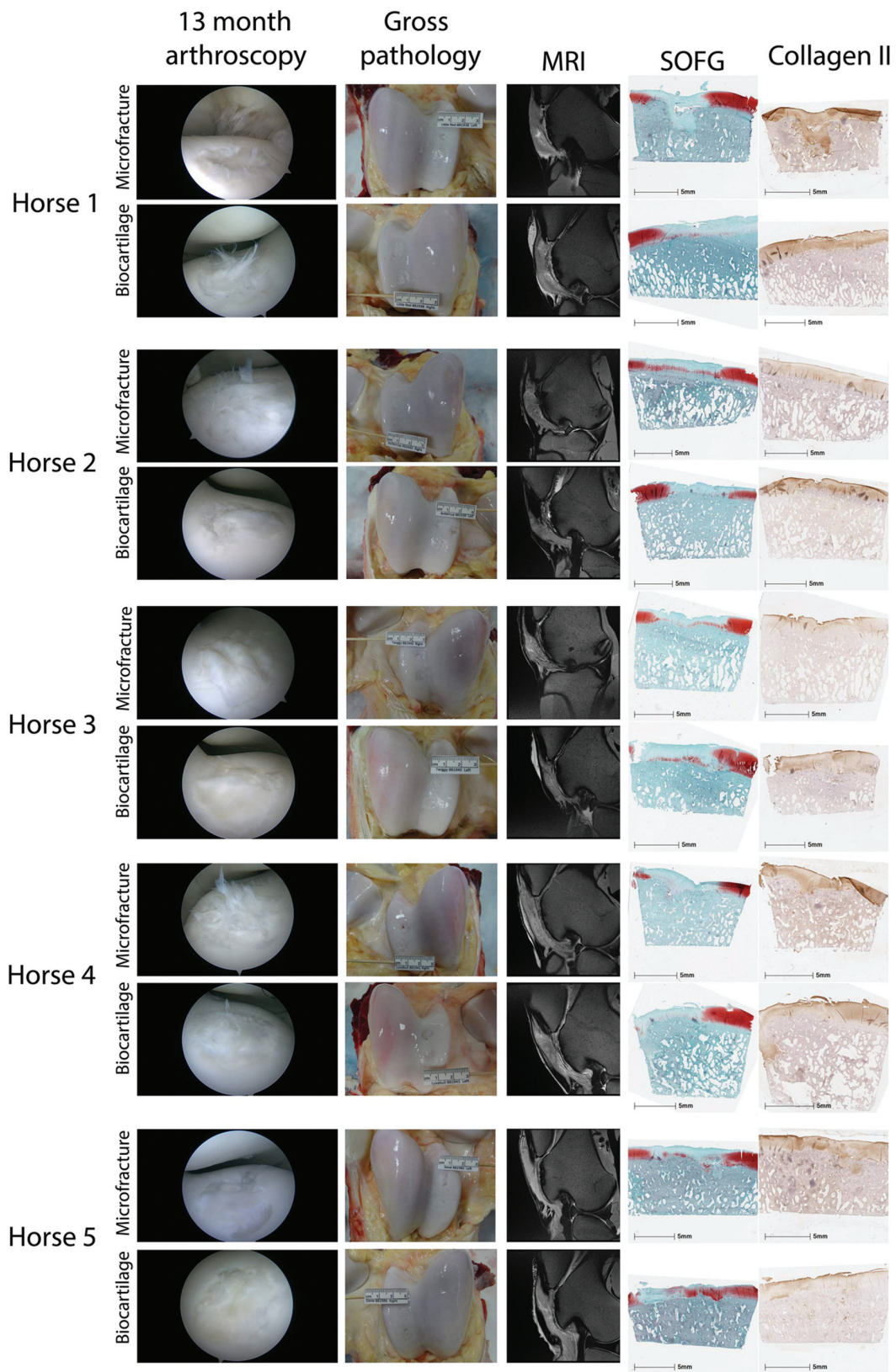
Figure 2. Arthroscopic images, safranin O–fast green (SOFG), and collagen type II immunohistochemistry of proximal defects from all 5 horses included in the study. Corresponding gross pathology photographs and morphologic sagittal plane 2-dimensional fast spin-echo magnetic resonance images (MRIs) from each limb. Scale bar = 5 mm.

TABLE 4
Significant Findings on Osteochondral Histologic Assessment of Repair Tissue Sites[a]

Histologic Category	BioCartilage	Microfracture	P Value
Repair-host integration (proximal)	96 ± 9	68 ± 18	.02
Basal integration (proximal)	100 ± 0	70 ± 37	.04
Subchondral bone at defect (proximal)	66 ± 18	34 ± 16	.05
Subchondral bone adjacent to defect (proximal)	100 ± 0	93 ± 11	.05
Type II collagen (proximal)	82 ± 8	58 ± 11	.05

[a]Data are reported as mean ± SD. The International Cartilage Repair Society II histologic scoring system was modified to capture change in subchondral bone architecture, with 100 being normal and indistinguishable from surrounding cartilage and 0 representing complete loss of normal architecture.

Micro-CT Evaluation

Trabecular thickness was not significantly different between MFx- and BioCartilage-treated defects ($P > .61$). The mean (±standard error) trabecular thickness ranged from a low of 0.34 ± 0.086 mm in BioCartilage-treated defects to a high of 0.38 ± 0.084 mm in distal MFx-treated defects. There was also no significant difference in trabecular spacing between groups or sites ($P \geq .47$), with mean values ranging from 0.13 ± 0.026 mm in distal MFx defects to 0.15 ± 0.040 mm in distal BioCartilage defects. Bone volume to tissue volume ratio was not significantly different between MFx and BioCartilage treatment groups ($P > .38$). The lowest ratio was calculated for a proximal BioCartilage-treated defect (0.59) and the highest for a distal MFx defect (0.83). Connectivity of the trabecular bone ranged from the lowest in the proximal MFx group (mean, 5.8 mm [1 ± 2.5]) and greatest in the proximal defects treated with BioCartilage (8.9 mm [1 ± 6.4]). There were no significant differences in connectivity between the groups or defect sites ($P \geq .23$). Osteophyte volume was not statistically different due to treatment or site ($P \geq .76$). Osteophyte volume showed the greatest range between defects and site. The largest mean osteophyte volume was found in the distal MFx-treated defects (60.2 mm [2 ± 46.0]), and the lowest mean volume was identified in proximal MFx defects (50.5 mm [2 ± 11.2]).

Histology

In synovial membrane tissues, no horses had inflammatory cell infiltrate or changes in villus architecture of their synovial membrane in either the BioCartilage- or MFx-treated limbs. This supports the arthroscopic scores and synovial fluid analysis results, which indicate that BioCartilage does not result in joint inflammation beyond that of arthroscopic surgery with MFx.

In repair sites, osteochondral bone blocks were evaluated histologically to capture changes in both the repair tissue and the subchondral bone. All significant findings were confined to the proximal, high-load lesions (Table 4). BioCartilage-treated proximal defects had significantly better scores for repair-host integration and base integration, and they formed more collagen type II than did the positive control defects (Figure 2). There were no significant differences between the groups for the distal defects for any of the score categories.

The implanted BioCartilage particles were not visible in any of the 20 defects. No epiphyseal or subchondral bone cysts, defined as a bone void with a true cyst lining, were present in either BioCartilage- or MFx-treated defects. Inflammatory cell infiltrates were not seen in the cartilage in any of the defects, and all defects had normal vascularization and cartilage calcification. No defect had completely normal surface architecture, matrix staining, or collagen type II formation.

DISCUSSION

These findings suggest that BioCartilage + PRP provides a safe and effective method for arthroscopic augmentation of MFx. BioCartilage + PRP was not associated with deleterious effects on the synovial fluid or synovial membrane of treated joints when compared with MFx alone in this 13-month-long large-animal study. Furthermore, there was no evidence of sepsis or synovial inflammation within any joint at 2-, 6-, or 13-month arthroscopies. At study end, BioCartilage + PRP had significantly better overall histologic scores for both defect sites compared with MFx controls, but no significant differences were noted between treatments with regard to repair tissue surface smoothness or integration with host cartilage.

MRI evaluation revealed that both treatments were associated with some abnormalities, including altered morphologic characteristics of repair cartilage, bone overgrowth, detachment of the subchondral plate, and sclerosis. One MFx defect had poor cartilage fill, while all the others were deemed to have good fill. All BioCartilage + PRP defects showed good fill on MRI. Both BioCartilage + PRP and MFx treatments resulted in a mixed signal intensity at the site of cartilage repair. This is consistent with immature repair tissue at the 13-month time point. Sclerosis was prevalent in all defects, and only 3 defects were devoid of bone overgrowth. T1ρ and T2 mapping were used to detect cartilage matrix degeneration/cartilage regeneration, with higher values corresponding to a higher degree of cartilage degeneration and lower amounts of cartilage regeneration. All joints had areas of higher and areas of lower values for both T1ρ and T2 mapping data sets. Overall, both treatments resulted in good fill of repair cartilage but had bone overgrowth, altered morphologic characteristics, and sclerosis of the repair cartilage. Only one of the BioCartilage +

PRP–treated defects was found to be well integrated into the surrounding tissue, while the remaining 19 defects showed moderate-poor integration. A lack of integration may predispose repair tissue to deterioration and loss of function over time due to increased exposure to shear forces elicited on the tissue.[8,9] Therefore, further optimization of this MFX-augmentation technique is desirable to positively affect long-term outcomes.

Four of the MFx control defects were found to be well integrated into the surrounding tissue. In the superficial half of repair tissue in distal defects, the T2 mapping was assessed as better in the BioCartilage + PRP group, suggesting improved collagen orientation. There was no significant difference between T1ρ mapping data sets for BioCartilage + PRP– and MFx-treated stifles, suggesting neither treatment was superior to the other with respect to increased glycosaminoglycan content.

Micro-CT allows for a nondestructive assessment and analysis of the 3D trabecular bone below the cartilage layer. There were some structural differences between the trabecular bone of the BioCartilage + PRP–treated defects and the MFx controls, but these were not statistically significant. These results indicate that BioCartilage + PRP does not appear to cause deterioration of the surrounding host tissue to any greater degree than MFx alone.

One limitation to this study is abnormal bone could not be compared with normal bone because a normal control was not included in the analysis. A further limitation was the lack of a phantom in the scanning procedure, thereby negating the use of bone mineral density measurements. Since these defects were solely full-thickness cartilage defects with minimal disruption to the subchondral bone, it is interesting to note the degree to which creating a chondral defect affects the underlying bone. Central osteophytes were present in both BioCartilage + PRP–treated joints and positive control joints, although no significant differences were noted. McCauley et al[6] describe an association between full-thickness or near-full-thickness cartilage defects with central osteophytes in naturally occurring disease in human knees. Similarly, Olive et al[11] describe central osteophytes deep to cartilage lesions in equine subjects. This finding may indicate the natural progression of healing in equine bone and cartilage in areas where immediate postoperative load could not be eliminated, leading to a bony response in addition to the bone healing response that is enhanced by performing the MFx technique in both groups. While this finding has been recorded, in both experimental models and naturally occurring disease, a correlation between severity of disease and osteophyte dimensions has not been published.

Finally, given the absence of a PRP- or fibrin sealant–only group, we cannot specify the relative contribution of these factors. The PRP and fibrin are used as carriers to hold the BioCartilage into the defect, and each or the combination of both could play a role in cartilage repair in addition to that provided by the BioCartilage.

The lack of subchondral and epiphyseal bone cysts in any defect is expected because the BioCartilage + PRP and MFx implantation surgery involved creation of only a full-thickness cartilage defect that did not break the subchondral bone plate. While no subchondral cysts were noted, subchondral bone voids were present in both groups, with only 3 defects having normal subchondral bone plate scores on histology. These voids and low subchondral plate scores could be remnants of the MFx awl perforations that did not resolve. All defects, except 2 positive control defects in the same limb, had normal subchondral plate scores adjacent to the defect.

Histologic assessment of the osteochondral blocks revealed all stifles in both BioCartilage + PRP and positive control treatment groups had altered cartilage and bone histology. Observed changes included altered surface architecture, altered matrix staining, formation of bone voids, subchondral plate disruption, and an incomplete fill of tissue into the defect. For distal defects, no statistical difference was seen in any category between treatment groups. BioCartilage + PRP was associated with significantly better repair-host integration, base integration, and collagen type II formation in the proximal defects. It has been suggested that the quality of cartilage, an increased collagen type II component in this case, is a stronger determinant of long-term outcome.[4] This implies that the use of BioCartilage + PRP in combination with MFx in cartilage defects may produce improved long-term outcome for patients when compared with MFx alone. However, the present study was only 13 months in duration, and additional studies are required to assess long-term outcome. On histology, there were no outcome parameters that were weaker in the BioCartilage + PRP group in comparison to the positive control group. There was no evidence of adverse reactions on terminal histology in either group.

A sample size of 5 in each group is a limitation to this study. Effect sizes for those tests that were significant are reported to provide the reader with an index to gauge the magnitude of the treatment effect.[3,14]

CONCLUSION

The osteochondral histology findings indicate that BioCartilage + PRP did not cause any adverse effects compared with the positive control and produced superior integration of repair tissue with more of the desired collagen type compared with MFx alone. The results up to 13 months after implantation indicate that BioCartilage + PRP is as safe as MFx for at least 13 months after implantation. When comparing data from MRI evaluation, micro-CT, synovial fluid cytology, synovial membrane histology, and bone and cartilage histology, there is no evidence of infection, inflammation, or other adverse effects related to the implanted device. There was no particulate material evident in any joint, and BioCartilage + PRP does not appear to cause deterioration of the surrounding host tissue. Arthroscopically, BioCartilage + PRP–treated cartilage defects produce better overall repair at least 13 months after implantation than does MFx alone. Histologically, BioCartilage + PRP produced better repair-host integration, base integration, and collagen type II in the proximal defects. These findings suggest that the repair seen in a full-thickness cartilage defect treated with BioCartilage

+ PRP is superior to treatment with MFx alone at 13 months. This result is particularly notable in higher load-bearing regions (i.e. proximal defects) where patellofemoral loads are highest.

ACKNOWLEDGMENT

REFERENCES

1. Abrams GD, Frank RM, Fortier LA, Cole BJ. Platelet-rich plasma for articular cartilage repair. *Sports Med Arthrosc*. 2013;21(4):213-219.
2. Abrams GD, Mall NA, Fortier LA, Roller BL, Cole BJ. BioCartilage: background and operative technique. *Oper Tech Sports Med*. 2013;21(2):116-124.
3. de Winter JCF. Using the Student's *t*-test with extremely small sample sizes. *Pract Assess Res Eval*. 2013;18(10):1-12.
4. Knutsen G, Drogset JO, Engebretsen L, et al. A randomized trial comparing autologous chondrocyte implantation with microfracture: findings at five years. *J Bone Joint Surg Am*. 2007;89(10):2105-2112.
5. Mainil-Varlet P, Van Damme B, Nesic D, Knutsen G, Kandel R, Roberts S. A new histology scoring system for the assessment of the quality of human cartilage repair: ICRS II. *Am J Sports Med*. 2010;38(5):880-890.
6. McCauley TR, Kornaat PR, Jee WH. Central osteophytes in the knee: prevalence and association with cartilage defects on MR imaging. *AJR Am J Roentgenol*. 2001;176(2):359-364.
7. McCormick F, Harris JD, Abrams GD, et al. Trends in the surgical treatment of articular cartilage lesions in the United States: an analysis of a large private-payer database over a period of 8 years. *Arthroscopy*. 2014;30(2):222-226.
8. Mithoefer K, McAdams T, Williams RJ, Kreuz PC, Mandelbaum BR. Clinical efficacy of the microfracture technique for articular cartilage repair in the knee: an evidence-based systematic analysis. *Am J Sports Med*. 2009;37(10):2053-2063.
9. Mithoefer K, Williams RJ III, Warren RF, et al. The microfracture technique for the treatment of articular cartilage lesions in the knee: a prospective cohort study. *J Bone Joint Surg Am*. 2005;87(9):1911-1920.
10. Moran CJ, Pascual-Garrido C, Chubinskaya S, et al. Restoration of articular cartilage. *J Bone Joint Surg Am*. 2014;96(4):336-344.
11. Olive J, D'Anjou MA, Girard C, Laverty S, Theoret CL. Imaging and histological features of central subchondral osteophytes in racehorses with metacarpophalangeal joint osteoarthritis. *Equine Vet J*. 2009;41(9):859-864.
12. Steadman JR, Rodkey WG, Singleton SB, Briggs KK. Microfracture technique for full-thickness chondral defects: technique and clinical results. *Oper Tech Orthop*. 1997;7:300-304.
13. Strauss EJ, Barker JU, Kercher JS, Cole BJ, Mithoefer K. Augmentation strategies following the microfracture technique for repair of focal chondral defects. *Cartilage*. 2010;1(2):145-152.
14. Sullivan GM, Feinn R. Using effect size: or why the P value is not enough. *J Grad Med Educ*. 2012;4(3):279-282.
15. Yanke AB, Chubinskaya S. The state of cartilage regeneration: current and future technologies. *Curr Rev Musculoskelet Med*. 2015;8(1):1-8.